American Journal of Transplantation 25 (2025) 476–488

Contents lists available at ScienceDirect

American Journal of Transplantation

journal homepage: www.amjtransplant.org

Original Article

Severe ischemia-reperfusion injury induces epigenetic inactivation of *LHX1* in kidney progenitor cells after kidney transplantation

Josep M. Cruzado [1,2,3,**], Anna Sola [2,11,12,†], Miguel L. Pato [4,5,†], Anna Manonelles [1,2,3], Cristian Varela [2], Fernando E. Setién [6], Carlos Quero-Dotor [6], James S. Heald [5], David Piñeyro [6,7], Ana Amaya-Garrido [2], Núria Doladé [2], Sergi Codina [1,2], Carlos Couceiro [1,2], Núria Bolaños [2], Montserrat Gomà [8], Francesc Vigués [3,9], Angelika Merkel [10], Paola Romagnani [11,12], María Berdasco [4,5,*]

[1] *Department of Nephrology, Hospital Universitari Bellvitge, Barcelona, Spain*
[2] *Nephrology and Renal Transplantation Group, Infectious Disease and Transplantation Program, Bellvitge Institute for Biomedical Research (IDIBELL), Barcelona, Spain*
[3] *Department of Clinical Sciences, University of Barcelona, Barcelona, Spain*
[4] *Cancer Epigenetics Group, Cancer Epigenetics and Biology Program (PEBC), Bellvitge Institute for Biomedical Research (IDIBELL), Barcelona, Spain*
[5] *Epigenetic Therapies Group, Genesis of Cancer Program, Josep Carreras Leukaemia Research Institute (IJC), Badalona, Spain*
[6] *Cancer Epigenetics Group, Genesis of Cancer Program, Josep Carreras Leukaemia Research Institute (IJC), Badalona, Spain*
[7] *Centro de Investigación Biomédica en Red Cáncer (CIBERONC), Madrid, Spain*
[8] *Department of Pathology, Hospital Universitari Bellvitge, Barcelona, Spain*
[9] *Department of Urology, Hospital Universitari Bellvitge, Barcelona, Spain*
[10] *Bioinformatics Unit, Josep Carreras Leukaemia Research Institute (IJC), Badalona, Spain*
[11] *Nephrology and Dialysis Unit, Meyer Children's Hospital, Scientific Institute for Research, Hospitalization and Healthcare (IRCCS), Florence, Italy*
[12] *Department of Biomedical, Experimental and Clinical Sciences "Mario Serio," University of Florence, Florence, Italy*

ARTICLE INFO

Keywords:
epigenetics

ABSTRACT

Severe ischemia-reperfusion injury (IRI) causes acute and chronic kidney allograft damage. As therapeutic interventions to reduce damage are limited yet, research on how to promote

Abbreviations: Ab, antibody; AKI, acute kidney injury; BAS, basiliximab; BMI, body mass index; DAPI, 4`,6-diamidino-2-phenylindole; DD, deceased donor; DD-KPC, kidney progenitor cell from a deceased donor; DE, differentially expressed; DEG, differentially expressed gene; DGF, delayed graft function; DMP, differentially methylated probe; DMR, differentially methylated region; eGFR, estimated glomerular filtration rate; ESRD, end-stage renal disease; F, female; FSGS, focal segmental glomerulosclerosis; GAPDH, glyceraldehyde-3-phosphate dehydrogenase; HLA, human leukocyte antigen; IRI, ischemia-reperfusion injury; LD, living donor; KPC, kidney progenitor cell; LD-KPC, kidney progenitor cell from a living donor; LHX1, LIM homeobox-1; M, male; mRNA, messenger RNA; MTT, 3-[4,5-dimethylthiazol-2-yl]-2,5 diphenyl tetrazolium bromide; N, no; NEG, negative; N-KPC, kidney progenitor cell derived from nephrectomy; POS, positive; PCR, polymerase chain reaction; PCX, podocalyxin; qPCR, quantitative polymerase chain reaction; rATG, rabbit antithymocyte globulin; RNA-seq, RNA-sequencing; RT, real-time; RT-PCR, real-time polymerase chain reaction; RT-qPCR, real-time quantitative polymesrase chain reaction; sh, short hairpin; TEC, tubular epithelial cell; U-KPC, urine-derived kidney progenitor cell; wt, wild-type; Y, yes.

* Corresponding author. María Berdasco, Epigenetic Therapies Group, Josep Carreras Leukaemia Research Center, Ctra de Can Ruti, Camí de les Escoles s/n Badalona (08916), Barcelona, Spain.
** Corresponding author. Josep M. Cruzado, Department of Nephrology, Hospital Universitari Bellvitge, C/Feixa Llarga, s/n, L'Hospitalet de Llobregat (08907), Barcelona, Spain.
E-mail addresses: jmcruzado@bellvitgehospital.cat (J.M. Cruzado), mberdasco@carrerasresearch.org (M. Berdasco).
† These authors contributed equally: Anna Sola and Miguel L. Pato.

https://doi.org/10.1016/j.ajt.2024.11.003
Received 6 June 2024; Received in revised form 16 October 2024; Accepted 1 November 2024
Available online 7 November 2024

gene expression
ischemia-reperfusion injury
kidney progenitor cells
kidney repair
kidney transplantation

kidney repair has gained significant interest. To address this question, we performed genome-wide transcriptome and epigenome profiling in progenitor cells isolated from the urine of deceased (severe IRI) and living (mild IRI) donor human kidney transplants and identified LIM homeobox-1 (*LHX1*) as an epigenetically regulated gene whose expression depends on the IRI severity. Using a mouse model of IRI, we observed a relationship between IRI severity, *LHX1* promoter hypermethylation, and *LHX1* gene expression. Using functional studies, we confirmed that *LHX1* expression is involved in the proliferation of epithelial tubular cells and podocyte differentiation from kidney progenitor cells. Our results provide evidence that severe IRI may reduce intrinsic mechanisms of kidney repair through epigenetic signaling.

1. Introduction

Ischemia-reperfusion injury (IRI) is associated with acute tubular necrosis after transplantation, causing a delay in recovery of kidney function that requires dialysis maintenance for days or weeks.[1,2] Moreover, severe IRI also induces podocyte damage and detachment.[33] The acute phase is followed by the activation of repair mechanisms that, depending on the severity of the damage, result in loss of nephrons, kidney allograft fibrosis, and progressive kidney allograft deterioration.[4]

IRI is inherent to the kidney transplantation procedure, and therapeutic interventions aimed at reducing kidney damage are very limited.[5] In this context, research on how to promote kidney repair has gained significant interest.[6,7] To date, multiple kidney cell populations showing stem cell-like properties have been described.[8,9] Most of these cells express the surface antigens CD24 and CD133, markers of adult kidney progenitor cells (KPCs). $CD133^{+}CD24^{+}$ cells can be isolated and expanded in vitro, where they can be differentiated into kidney-specific cells (podocytes and tubular cells).[10] Injection of $CD133^{+}CD24^{+}$ cells in a model of acute kidney injury (AKI) in severe combined immunodeficient mice resulted in tubular regeneration at different portions of the nephron.[10] In contrast to this regenerative role, it has been described that parietal glomerular $CD133^{+}CD24^{+}$ cell activation and proliferation is involved in the pathogenesis of rapidly progressing glomerulonephritis and focal and segmental glomerulosclerosis.[11,12]

The discovery of $CD133^{+}CD24^{+}$ urine-derived KPCs (U-KPCs) represents an opportunity for translational research using a noninvasive procedure.[13,14] U-KPCs have been seldom identified in physiological conditions (eg, pregnancy) but usually in kidney diseases, including glomerular diseases and kidney transplantation.[15,16] Interestingly, CD133+CD24+ cells were transiently detected in urine in all patients during the first week after transplantation, but only those patients maintaining U-KPCs after 6 months of transplantation showed estimated glomerular filtration rate decline, developed proteinuria and chronic allograft damage.[16] Although some gene expression patterns have been identified for murine KPCs in some glomerulopathies,[17] a complete profiling of human U-KPCs under different pathologic conditions is still lacking. Epigenetic mechanisms governing gene expression will contribute to defining the molecular pathways determining the regenerative or prosclerotic role of KPCs in disease.

In this work, we focused on the molecular profiling of human U-KPCs obtained from kidney allograft recipients early after transplantation, depending on the severity of IRI. We proposed that alterations in the epigenetic mechanisms due to the exposition to IRI underpin the changes underlying causes of the gene expression and could consequently provide a molecular explanation of the U-KPC heterogeneity and response to injury. To address this question, we performed high-throughput RNA-sequencing (RNA-seq) and genome-wide 5`—C—phosphate—G—3` (CpG) methylation arrays of U-KPCs obtained from recipients of a deceased donor kidney (maximal severe IRI) and recipients of a living donor kidney (mild injury). Functional analysis of proliferation and differentiation in in vitro models was performed based on candidate genes.

2. Materials and Methods

2.1. Study population

The study population consisted of kidney transplant recipients from deceased or living donors between 2016 and 2019 (Supplementary Fig. S1). Clinical data of the discovery and validation cohorts are summarized in Tables 1 and 2, respectively. KPC isolation from U-KPCs was performed as described previously.[10] Briefly, urine samples were collected between days 2 and 7 after transplantation. CD133+ and CD24+ positive cells were selected using fluorescence-activated cell sorting analysis. As controls for U-KPCs, we used KPCs isolated from adult human nephrectomies (N-KPCs). The details for the isolation and characterization of cultured U-KPC and N-KPC are presented in Supplementary Text 1.

2.2. Human leukocyte antigen typing

Human leukocyte antigen (HLA) typing was performed using sequence-specific oligonucleotide polymerase chain reaction (PCR) using bead arrays on a Luminex platform (Lifecodes, Immucor, Stamford, CT). Only patients having U-KPCs from donor origin were considered for molecular analysis.

Table 1
Discovery set.

Variable	DD n = 27	LD n = 11	*P*-value
Donor age (y)	58.9 ± 13.3	49.0 ± 12.4	.06
Donor sex (M/F)	16/11	6/5	.97
Recipient age (y)	55.6 ± 13.9	45.8 ±14.0	.06
Recipient gender (M/F)	15/12	6/5	.95
BMI (kg/m^2)	25.9±4.9	25.3 ± 5.8	.57
Dialysis time (mo)	42.3 ± 35.7	3.2 ± 5.8[a]	< .001
Cause of ESRD			.71
Diabetes	3	1	
Glomerular disease	7	3	
Hereditary	2	1	
Hypertension	3	0	
Interstitial	5	2	
Unknown	7	4	
Previous transplant (Y/N)	7/20	2/9	.39
HLA mismatch	3.9 ± 1.2	3.7 ± 1.1	.45
AntiHLA Ab (POS/NEG)	10/17	2/9	.23
Induction (BAS/rATG)	16/11	8/3	.54
Cold ischemia time (h)	16.2 ± 6.5	0.7 ± 0.4	< .001
DGF (Y/N)	12/15	0/11	.03
Serum creatinine level 1 wk (μmol/L)	242 ± 183	110 ± 25	.02
eGFR 3 mo (mL/min)	46 ± 14	63 ± 17	.005
eGFR 1 y (mL/min)	51 ± 16	64 ± 16	.04

No patients suffered from acute rejection.
All patients are receiving tacrolimus, mofetil mycophenolate, and steroids.
Ab, antibody; BAS, basiliximab; BMI, body mass index; DD, deceased donor; DGF, delayed graft function; eGFR, estimated glomerular filtration rate; ESRD, end-stage renal disease; F; female; HLA, human leukocyte antigen; LD, living donor; M, male; N, no; NEG, negative; POS, positive; rATG, rabbit antithymocyte globulin; Y, yes.

[a] Six out of 11 received preemptive kidney transplantation.

Table 2
Validation set.

Variable	DD n = 16	LD n = 18	*P*-value
Donor age (y)	60.7 ± 19.6	55.2 ± 10.9	.31
Donor gender (M/F)	10/6	7/11	.30
Recipient age (y)	59.3 ± 15.5	51.4 ± 13.2	.12
Recipient sex (M/F)	10/6	12/6	1.00
BMI (kg/m^2)	27.7 ± 4.3	24.1 ± 4.4	.02
Dialysis time (mo)	40.9 ± 38.4	2.7 ± 5.5[a]	.001
Cause of ESRD			.20
Diabetes	2	0	
Glomerular disease	6	9	
Hereditary	0	3	
Hypertension	1	0	
Interstitial	4	2	
Unknown	3	4	
Previous transplant (Y/N)	2/14	2/16	1.00
HLA mismatch	4.4 ± 1.2	3.8 ± 1.7	.25
AntiHLA Ab (POS/NEG)	5/11	1/17	.08
Induction (BAS/rATG)	10/5/1	17/0/1	.04
Cold ischemia Time (h)	16.3 ± 7.7	1.1 ± 1.1	< .001
DGF (Y/N)	5/11	0/18	.01
Serum creatinine level 1 wk (μmol/L)	189 ± 165	102 ± 26	.05
eGFR 3 mo (mL/min)	46 ± 20	57 ± 17	.09
eGFR 1 y (mL/min)	49 ± 23	61 ± 19	.09

No patients suffered from acute rejection.
All patients receiving tacrolimus, mofetil mycophenolate, and steroids.
Ab, antibody; BAS, basiliximab; BMI, body mass index; DD, deceased donor; DGF, delayed graft function; eGFR, estimated glomerular filtration rate; ESRD, end-stage renal disease; F; female; HLA, human leukocyte antigen; LD, living donor; M, male; N, no; NEG, negative; POS, positive; rATG, rabbit antithymocyte globulin, Y, yes.

[a] Twelve out of 18 received a preemptive kidney transplantation.

2.3. RNA-seq analysis

Total RNA from CD133+CD24+ cells was extracted on a Maxwell RSc device. A total of 5 μg RNA from each sample was used for RNA-seq analyses following the TruSeq Stranded messenger RNA (mRNA) sequencing method (Illumina). The details for RNA-sequencing processing and data analysis are presented in Supplementary Text 1.

2.4. DNA methylation microarrays

DNA was extracted using conventional phenol:-chloroform:isoamyl alcohol (Sigma). Bisulfite modification of 600 ng genomic DNA was carried out with the EZ DNA Methylation Kit (Zymo) following the manufacturer's protocol. Genome-wide CpG methylation was quantified using the Infinium MethylationEPIC (EPIC) BeadChip (Illumina). The details for DNA methylation processing and data analysis are presented in Supplementary Text 1.

2.5. LIM homeobox-1 promoter methylation and gene expression

For validation studies, we used an independent cohort of cultured U-KPCs (Fig. 1 and Table 2). LIM homeobox-1 (*LHX1)* differential methylation was performed using pyrosequencing analysis. LHX1 expression analysis was determined using quantitative PCR (qPCR). The detailed protocols are presented in Supplementary Text 1.

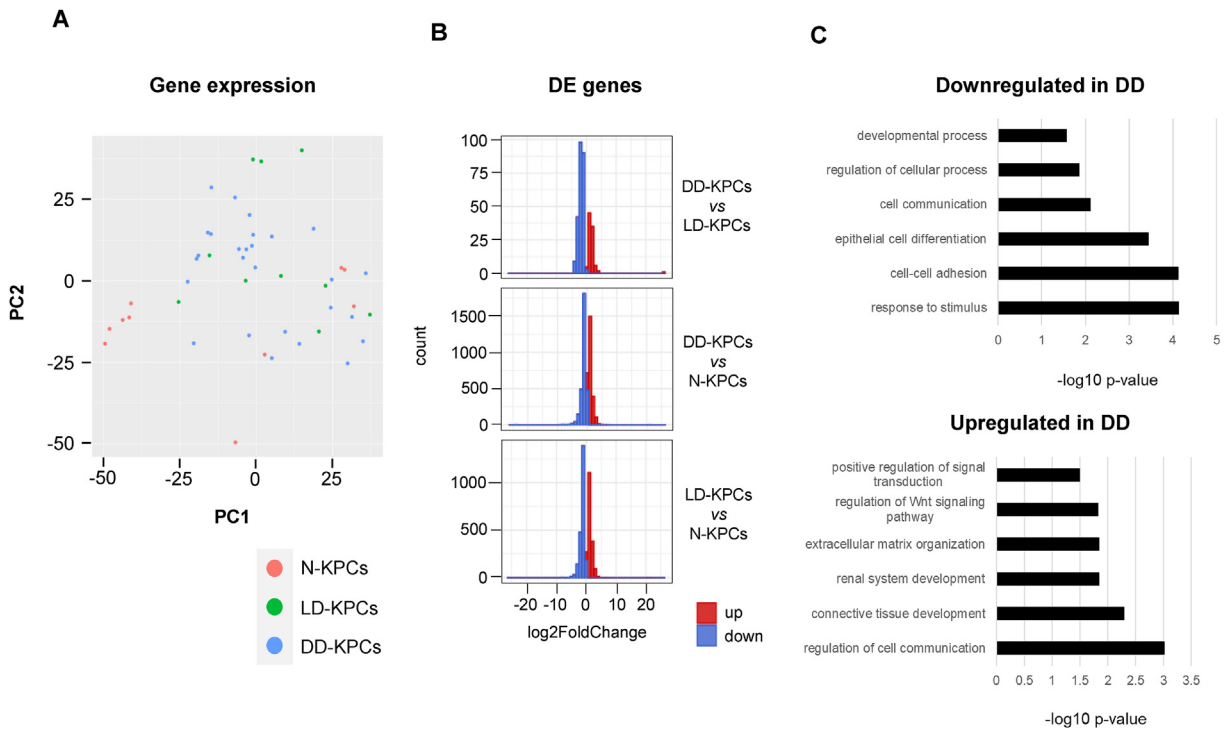

Figure 1. Transcriptome studies of urine-derived kidney progenitor cells (KPCs) (U-KPCs) from living or deceased donor kidney transplant recipients. (A) Principal component analysis for gene expression results obtained from RNA-sequencing. Shown are all 3 pairwise comparisons between U-KPCs from a deceased donor (DD) KPCs (DD-KPCs) or living donor (LD) KPCs (LD-KPCs) origin and kidney progenitor cells taken from nephrectomy KPCs (N-KPCs). (B) Expression changes in differentially expressed (DE) genes. (C) Gene ontology enrichments (biological function) among the DE genes whose expression differs between DD-KPCs and LD-KPCs.

2.6. Confocal imaging of kidney allograft biopsies

LHX1 protein detection using immunofluorescence was performed in 6 kidney allograft biopsies per group obtained 10 days after transplantation with a pathologic diagnosis of "pure" acute tubular necrosis. The details for the immunofluorescence method and imaging processing are presented in Supplementary Text 1.

2.7. Mouse model of IRI

Two different animal models of ischemia in C57BL/6 mice were performed. In the first one, ischemia was induced using bilateral clamping of renal blood vessels for 30 minutes and sacrificed at 24 to 72 hours. In the second model, ischemia was induced using clamping of the left renal blood vessels for 15, 30, 45, or 60 minutes while the right kidney was removed to simulate kidney transplantation. Mice were sacrificed at 24 hours. The severity of AKI was assessed using blood urea nitrogen (BUN) and serum creatinine levels as detailed in Supplementary Text 1. Molecular characterization of LHX1 mRNA and protein expression and *LHX1* promoter methylation methods are detailed in Supplementary Text 1.

2.8. LHX1 cloning and transfection

The wild-type (wt) *LHX1* coding sequence and a mutant isoform lacking the DNA binding motif were cloned into a pLVX-IRES vector (Clontech) and transfected into HEK293T cells. Viral vectors were transfected into Caki2 or U-KPC cells. Positive clones were sorted using flow cytometry and cultured for the estimation of cell proliferation. The details of the cloning and transfection methods, Western blotting, 3-[4,5-dimethylthiazol-2-yl]-2,5 diphenyl tetrazolium bromide analysis, and colony-formation assays are presented in Supplementary Text 1.

2.9. In vitro induction of podocyte differentiation from KPCs

Control and transfected KPCs were differentiated into podocyte lineages as described previously.[16] Briefly, cells were incubated for 72 hours with VRAD medium (DMEM/F12 [Sigma-Aldrich, St. Louis, MO], 10% fetal bovine serum [Hyclone)], 100 nM vitamin D3, and 100 mM retinoic acid). Differentiation was evaluated using mRNA quantification (using qPCR) and protein detection (using immunofluorescence) (detailed in Supplementary Text 1).

2.10. LHX1 stable silencing

HEK293T cells were transfected with *LHX1*-specific short hairpin RNA (sh RNA or scrambled shRNA in the pLVX-shRNA2 vector (Clontech). Supernatants containing the viral vectors were transfected in Caki1 cells for cell proliferation assays. The details of the transfection method, Western blotting for LHX1, and cell proliferation analysis are presented in Supplementary Text 1.

2.11. Statistical analysis

Comparisons of clinical parameters were made between deceased and live donor kidney transplantation. The differences between the 2 groups for continuous variables were analyzed using the nonparametric Mann-Whitney U test. The differences between categoric variables were analyzed using the Fisher exact test. All statistical tests were considered significant if the *P*-value was $< .05$ for 2-tailed tests. The statistical analysis was performed with the StatView SAS program.

3. Results

3.1. Decreased global gene expression in urine kidney progenitor cells from deceased donor transplantation

To study whether U-KPCs after kidney transplantation differ in their transcriptomes depending on the donor condition and IRI severity, we performed RNA-seq on U-KPCs from recipients with deceased donors KPCs (DD-KPCs) or living donors KPCs (LD-KPCs) transplantation (Supplementary Fig. S1 and Table 1). Although short-term culture expansion, a prerequisite to achieving enough KPCs for high-throughput analysis, can impact the gene expression and epigenetic profiles, we assume that DD-KPCs and LD-KPCs were equally affected. Furthermore, we also include in the analysis KPCs isolated directly from nephrectomy tissue (N-KPCs) to compare with the transcriptome of progenitor stem cells found in primary kidney tissue. Global gene expression patterns from DD-KPCs or LD-KPCs were closely related, and principal component analysis did not segregate sample groups depending on the donor origin (Fig. 1A). Differential expression analysis (*P*-adjusted $< .05$) revealed 333 genes with differential expression between DD-KPCs or LD-KPCs (Supplementary Table 1) with a clear tendency to downregulation in DD-KPCs (236 and 79 genes were downregulated or upregulated in DD, respectively) (Fig. 1B). Gene ontology enrichment of the differentially expressed genes (DEGs) in DD-KPCs revealed biological functions associated with loss of renal differentiation and increased expression of profibrotic genes (Fig. 1C), which correlates with the well-described alterations after IRI. As expected, the integration of transcriptome data from U-KPCs and N-KPCs revealed gene expression differences depending on the tissue of origin (Fig. 1B). The most interesting observation was that global gene expression patterns of LD-KPCs resembled closer gene expression profiles of N-KPCs than those of DD-KPCs. Specifically, we found 3933 DEGs between LD-KPCs and N-KPCs and 5246 DEGs between DD-KPCs and N-KPCs. Data showed that the higher IRI severity associated with DD transplantation results in increased changes in gene expression.

3.2. Increased genome-wide DNA methylation in U-KPCs from DDs

The genomic DNA of DD-KPCs, LD-KPCs, and N-KPCs was interrogated for their DNA methylation landscape using the Infinium EPIC microarray. Principal component analysis captures the N-KPCs sample group but does not enable further segregation of the remaining KPCs samples, indicating that the global methylation profiles do not strongly differ between DD-KPCs and LD-KPCs (Fig. 2A). The analysis of differentially methylated probes (DMPs) (adjusted *P*-value $< .05$; mean methylation differences $> .1$) revealed 1687 DMPs between DD-KPCs and LD-KPCs (Supplementary Table 2). Hypermethylation in DD-KPC samples was higher than hypomethylation events (1326 and 361 DMPs were found, respectively) (Fig. 2B). This gain of CpG methylation in DD-KPCs is consistent with the higher downregulation of gene expression observed for DD-KPCs samples (Fig. 1B). Global DNA methylation (defined as the median methylation levels per sample considering all probes) was also significantly higher in DD-KPCs compared with LD-KPCs (Wilcoxon rank sum test: *P*-value $= .04384$) (Fig. 2C). Regarding the genomic context, methylation differences between DD- and LD-KPCs were mainly found at intragenic regions and gene bodies in CG-poor regions ("open sea") (Fig. 2D). A significant proportion of DMPs found between U-KPCs (both DD and LD) and N-KPCs were distributed in CG-rich regions (at CpG islands and shelves) and coincided with regulatory regions (Fig. 2D), reflecting tissue-dependent CpG methylation.

Because DNA methylation data are strongly correlated between nearby CpG-sites, we also tested for differentially methylated regions (DMRs). We found 8 DMRs hypermethylated in DD-KPCs and only 1 DMR hypomethylated in DD-KPCs (Supplementary Fig. S2). Interestingly, the list was enriched in transcription factors and other regulatory proteins with a defined role in tissue development, including kidney differentiation and homeostasis (Supplementary Table 3).

3.3. Epigenetic silencing of the LHX1 kidney-specification gene is associated with IRI

Next, we wondered whether an overlap of DEGs and DMRs between DD-KPCs and LD-KPCs exists to indicate epigenetic silencing. Results showed that the *LHX1* gene met both criteria: it showed a DMR with higher methylation (Fig. 3A) and lower gene expression (Fig. 3B) in recipients with a DD transplant. Accordingly, we also observed a significant negative correlation (Pearson coefficient $= -0.66$, $P < .001$) between mean DMR methylation and gene expression for *LHX1* (Fig. 3C). To further demonstrate the epigenetic regulation of *LHX1* expression, we cultured hypermethylated human KPCs with the addition of the DNA methylation inhibitor 5-azacytidine (1 μM for 72 hours), which resulted in increased *LHX1* gene expression (Fig. 3D).

To confirm molecular differences, we used a validation cohort of patients (Table 2). The pyrosequencing analysis confirmed a significant increase in *LHX1* hypermethylation in DD-KPCs (Fig. 3E) (unpaired t-test, two-tailed, *P*-value $= .0008$). We also observed that *LHX1* gene expression was different between DD-KPCs and LD-KPCs (unpaired t-test, 2-tailed, *P*-value $= .099881$) but it should be highlighted that high intragroup variability was detected (Fig. 3F). Furthermore, to study *LHX1* expression in an in vivo human model and to avoid the epigenetic drift potentially associated with cultured cells, we decided to use transplant kidney biopsies obtained in the first 10 days after

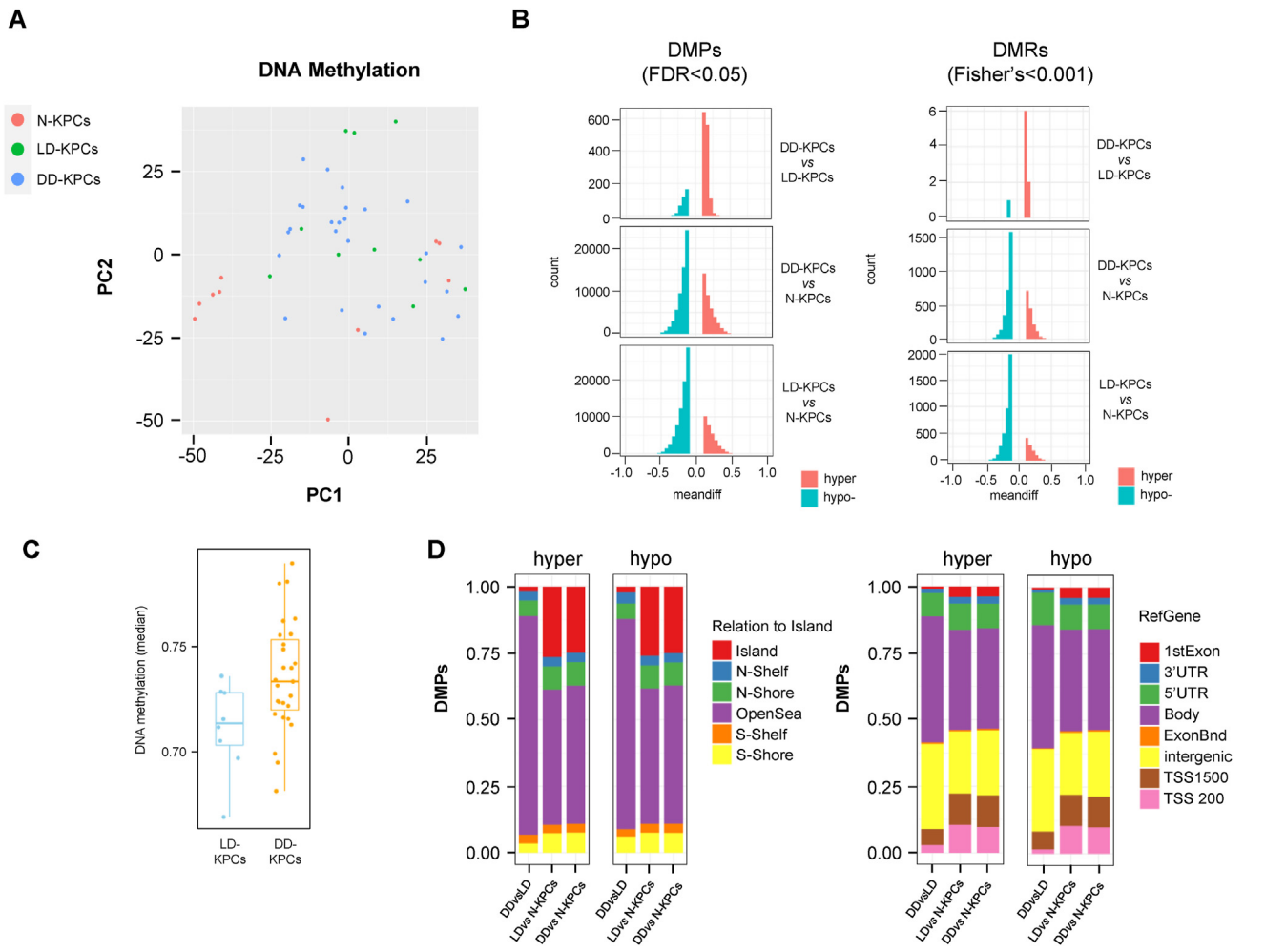

Figure 2. Epigenome-wide studies of urine-derived kidney progenitor cells (KPCs) (U-KPCs) from a living donor (LD) or deceased donor (DD) kidney transplant recipients. (A) Principal component analysis for DNA methylation results obtained from the Infinium MethylationEPIC array. Shown are all 3 pairwise comparisons between U-KPCs from DD-KPCs or LD-KPCs origin and KPCs taken from nephrectomy (N-KPCs). (B) Left, methylation changes in differentially methylated 5`—C—phosphate—G—3`s (CpGs)/probes (DMPs); right, methylation changes in differentially methylated regions (DMRs). (C) Overall CpG methylation levels per sample in DD-KPCs and LD-KPCs (measured as the median of all probes). (D) Distribution of DMPs for all 3 pairwise comparisons (DD-KPCs, LD-KPCs, and N-KPCs) according to CpG content (left) and functional genomic distribution (right).

kidney transplantation. We assessed whether the expression of LHX1 protein in CD133+ cells differed in allograft biopsies depending on the LD or DD origin. Results showed that the percentage of LHX1 protein expression in CD133-positive cells was significantly higher in LD biopsies than in DD biopsies (unpaired t-test, 2-tailed, *P*-value = .0039) (Fig. 3G). The representative images by immunofluorescence confirmed that the LHX1 protein expression in CD133-positive cells was more abundant in biopsies from LD compared with DD tissues both in tubular and glomerular cells (Fig. 3H).

3.4. Kidney expression of LHX1 in mouse models of IRI

Immunohistochemistry analysis showed that LHX1 was mainly expressed in glomerular parietal epithelial cells, podocytes, and proximal tubular epithelial cells (Supplementary Fig. S3A). We observed that after IRI, LHX1 expression was associated with the severity of acute kidney injury (Supplementary Fig. S3A, B). Furthermore, kidney *LHX1* mRNA expression was associated with the number of positive glomerular and tubular cells (Supplementary Fig. S3C). In the experimental model of IRI with several times of warm ischemia (0, 15, 30, 45, and 60 minutes), we demonstrated a relationship between warm ischemia time, renal dysfunction (Fig 4A, B), *LHX1* promoter hypermethylation (Fig. 4C), and *LHX1* gene expression (Fig. 4D).

3.5. Role of LHX1 in KPC differentiation

To strengthen the link between *LHX1* expression and kidney organogenesis in human models, we reconstituted *LHX1* function in KPCs showing low *LHX1* expression. We designed 2 *LHX1* isoforms: a wt *LHX1* isoform (LHX1wt) and a mutant *LHX1* isoform lacking the DNA binding motif (LHX1mut); the latest was used as a negative control with a similar size to wt construction but nonfunctional (Fig. 5A).[18] Increased mRNA and protein levels in the ectopically LHX1-expressing cells in comparison with the endogenous levels in the control cells are shown in Figure 5B. After 21 days of subculture, cells showing

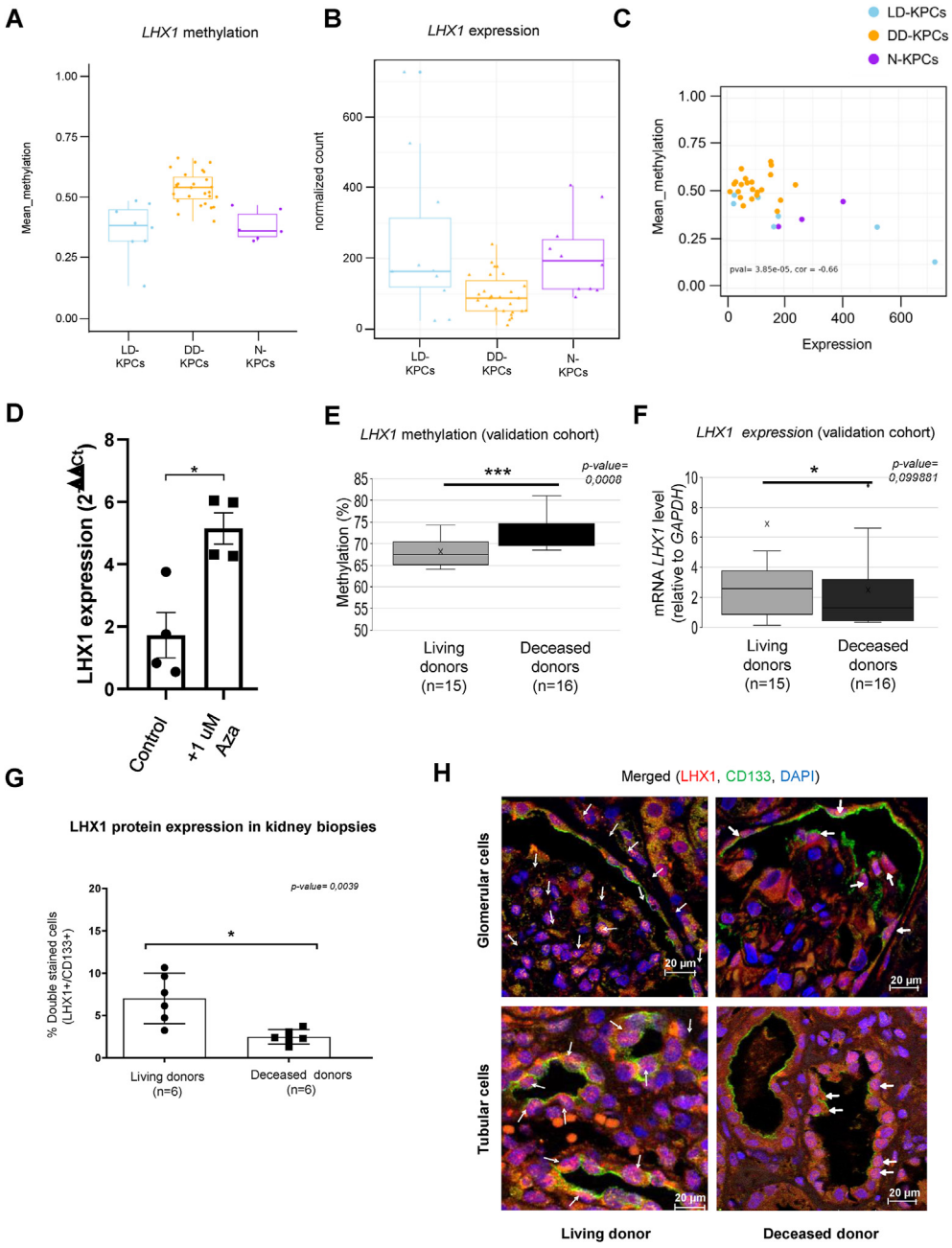

Figure 3. Epigenetic-regulated expression of LIM homeobox-1 (LHX1) in urine-derived kidney progenitor cells (KPCs) (U-KPCs) and protein LHX1 expression in human kidney biopsy samples. (A) Boxplot showing mean *LHX1* DNA methylation per sample per group, including KPCs from nephrectomy KPCs (N-KPCs) and U-KPCs from living donor (LD) transplants (LD-KPCs) or deceased donor (DD) transplants (DD-KPCs). Data correspond to β-values obtained from the Infinium MethylationEPIC array of the discovery cohort. (B) *LHX1* gene expression per sample by group, including N-KPCs, LD-KPCs, and DD-KPCs. Data correspond to processed raw reads obtained from RNA-sequencing analysis of the discovery cohort. (C) Correlation between *LHX1* mean DNA methylation and *LHX1* gene expression per sample by group, including N-KPCs, LD-KPCs, and DD-KPCs. (D) Treatment with the demethylating agent 5-azacitidine (5-Aza; 1 µM for 72 hours) reactivates *LHX1* gene expression in *LHX1*-hypermethylated KPC cell lines. Statistical significance was determined using a 1-way analysis of variance test with Tukey's multiple comparison test, $*P < .05$. (E) Promoter methylation of the *LHX1* gene in a validation cohort of U-KPCs (LD-KPCs and DD-KPCs). Bars show the percentage of DNA methylation from 0 to 100 obtained using pyrosequencing. (F) Real-time (RT) polymerase chain reaction (PCR) (RT-PCR) expression levels of the *LHX1* gene in a validation cohort of U-KPCs (LD-KPCs and DD-KPCs). *LHX1* messenger RNA (mRNA) expression relative to glyceraldehyde-3-phosphate dehydrogenase was detected using RT-quantitative PCR. (G) Quantification of LHX1-positive nuclei in CD133-positive cells in kidney allograft biopsies from deceased and living donors. (H) Representative images (63 ×) of the immunofluorescence staining for 4`,6-diamidino-2-phenylindole (DAPI) (blue), CD133 (green), and LHX1 (red) in kidney allograft biopsies from DDs and LDs. Results on tubular and glomerular cells are shown. Arrows indicate double-stained cells. Negative controls included nonspecific immunoglobulin and no primary antibody (data not shown). Scale bar = 20 µm. Statistical significance was determined using a paired t-test, 2-tailored, $*P < .05$; $***P < .0$.

LHX1 overexpression showed alterations in the cell morphology. Although nontransfected and mutant-transfected cells (pLVX-LHX1mut) appear as simple ultrastructure with a simple elongated shape, the wt transfected cells (pLVX-LHX1wt) acquire a markedly elongated shape with finger-like projections (Supplementary Fig. S3). These changes in cell morphology that resemble the foot processes of podocytes prompted us to analyze whether *LHX1* overexpression favors a spontaneous differentiation of in vitro KPCs to podocytes. We observed that pLVX-LHX1wt transfection induces spontaneous differentiation to podocytes assessed using mRNA of the podocalyxin marker, whereas pLVX-LHX1mut cells retain undifferentiated properties assessed using quantification of mRNA CD133 expression (Fig. 5C). To validate this observation, we grew KPCs under a podocyte differentiation protocol based on exposing primary KPCs to all-trans retinoic acid in a VRAD medium. We confirmed that pLVX-LHX1wt transfected cells differentiated earlier than pLVX-LHX1mut or control cells (Fig. 5D, E). Podocalyxin strongly increases at 72 hours of subculture in the podocyte-induction medium in the pLVX-LHX1wt, together with a decreased expression of the CD133 progenitor marker. In summary, our results confirm that *LHX1* overexpression strongly favors podocyte differentiation of cultured KPCs.

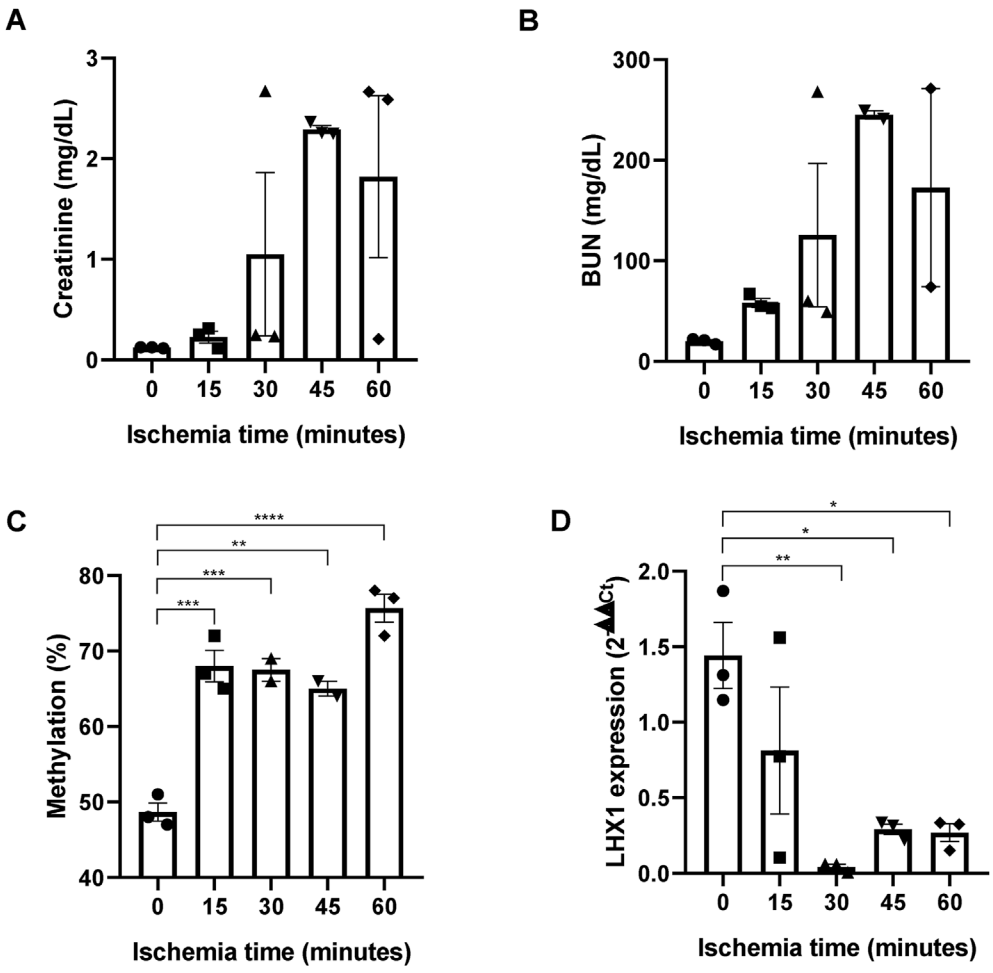

Figure 4. Renal warm ischemia induces methylation and LIM homeobox-1 (*LHX1)* downregulation in a mouse model of ischemia-reperfusion injury (IRI). (A) Serum creatinine levels; (B) blood urea nitrogen (BUN) levels; (C) kidney *LHX1* methylation levels, and (D) *LHX1* messenger RNA (mRNA) expression of mice subjected to nephrectomy and ischemia of 0, 15, 30, 45, or 60 minutes. Statistical significance was determined using a 1-way analysis of variance test with Tukey's multiple comparison test, $^{*}P < .05$; $^{**}P < .01$ $^{***}P < .001$; $^{****}P < .0001$.

3.6. Role of LHX1 expression in cellular proliferation of kidney tubular epithelial cells

During recovery from IRI, nondamaged tubular epithelial cells can dedifferentiate and proliferate, favoring cellular repair.[19] Given that we also observed LHX1 expression in tubular epithelial cells (Fig. 3G), we proposed to study its role in promoting their proliferation. Due to methodologic limitations of prolonged culture expansion of primary proximal tubular epithelial cells, we employed human kidney cell lines that have previously been validated as a well-differentiated polarized proximal tubule cell in vitro, regardless of its cancerous origin and multiple passaging.[20] We quantified *LHX1* mRNA expression in a panel of commercially available renal cell lines and observed that Caki-1 exhibits a higher expression of *LHX1,* whereas Caki-2 showed the lowest *LHX1* mRNA levels (Supplementary Fig. S4). We adopted a double approach for proliferation studies. First, we performed pLVX-LHX1wt transfection in Caki-2 cells. Upon restoration of LHX1 expression, as demonstrated using RT-PCR and western blotting analyses (Fig. 6A), the Caki-2 cell line experienced increased cell growth in 3-[4,5-dimethylthiazol-2-yl]-2,5 diphenyl tetrazolium bromide-proliferation assays as well as in colony-formation assays (Fig. 6B, C). Cells transfected with the pLVX-LHX1mut vector did not show any increase neither in cell proliferation nor colony-formation ability compared with empty vector-transfected cells (Fig. 6B, C; analysis of variance test, *P*-value $< .05$). Second, we also knocked down *LHX1* expression using stable RNA interference (shRNA) in the Caki-1 renal cell line. mRNA and protein LHX1 levels were reduced in shLHX1 cells compared with wt cells (Fig. 6D). We observed that significantly reduced LHX1 expression was associated with decreased cell growth and a reduction in the colony-formation ability compared with scrambled transfected cells (Fig. 6E, F, analysis of variance test, *P*-value $< .05$). Altogether, results indicate that LHX1 expression in human renal epithelial tubular cells is associated with increased cellular proliferation.

4. Discussion

The main finding from this study is that severe IRI induces DNA hypermethylation in KPCs isolated from urine early after kidney transplantation. These epigenetic changes are associated with global gene expression changes, mostly resulting in the downregulation of molecular pathways linked to kidney development, epithelial cell differentiation, and cell adhesion. We identified the *LHX1* gene, a well-known transcription factor involved in early kidney development,[21,22] as a potential candidate for repair dysregulation after IRI. LHX1 is expressed mainly in glomerular parietal epithelial cells, podocytes, and tubular epithelial cells and decreases after severe IRI. Functional studies

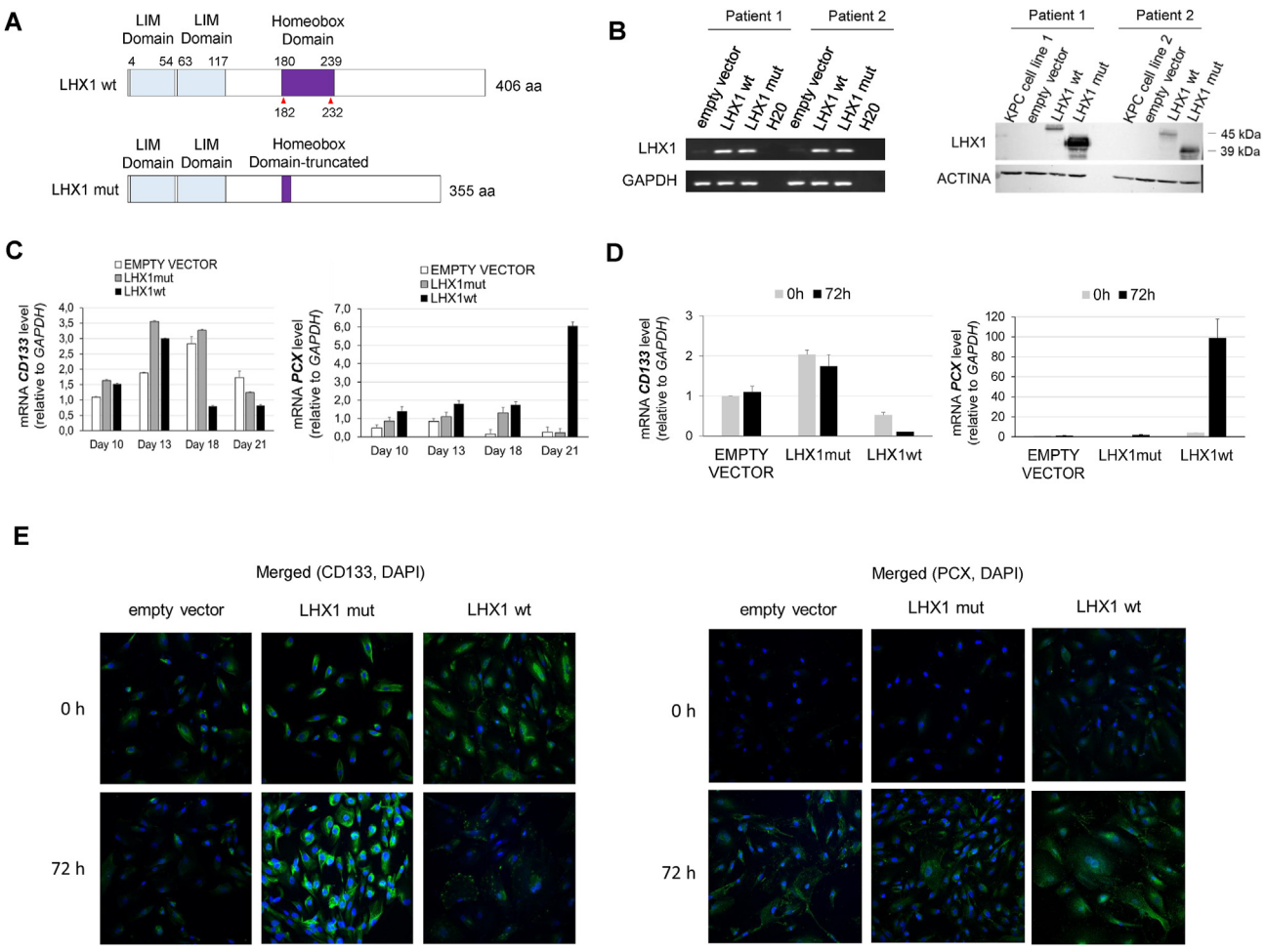

Figure 5. LIM homeobox-1 (LHX1) overexpression induces in vitro differentiation of kidney progenitor cells (KPCs). (A) Schematic illustration of the experimental workflow to induce upregulation of LHX1 in cultured KPCs. Two LHX1 isoforms were used for the transaction assays: a mutant LHX1 isoform lacking the DNA binding motif (LHX1mut) and a wt LHX1 isoform (LHX1wt). (B) LHX1 expression was monitored using quantitative polymerase chain reaction (qPCR) (left) and western blot (right) in LHX1mut- and LHX1wt-transfected KPCs. (C) Messenger RNA (mRNA) expression levels of the progenitor renal cell biomarker CD133 (left) and the podocyte biomarker podocalyxin (PCX) (right) relative to glyceraldehyde-3-phosphate dehydrogenase (GAPDH) were detected using real-time qPCR (RT-qPCR) in nontransfected and transfected (LHX1mut and LHX1wt) KPCs after 21 days of subculture in standard culture medium. Three biological replicates were performed per condition. Data are expressed as mean ± SD. (D) mRNA expression levels of the progenitor renal cell biomarker CD133 (left) and the podocyte biomarker PCX (right) relative to GAPDH were detected using RT-qPCR in nontransfected and transfected (LHX1mut and LHX1wt) KPCs after 72 hours of subculture in podocyte-induction culture medium. Three biological replicates were performed per condition. Data are expressed as mean ± SD. (E) Representative images (25 ×) of the immunofluorescence staining of CD133 (left) and PCX (right) proteins in nontransfected and transfected (LHX1mut and LHX1wt) KPCs after 72 hours of growth in podocyte-induction culture medium.

demonstrated a dual role of LHX1 in kidney response after damage. First, LHX1 overexpression in KPCs induces podocyte differentiation, and second, expression of LHX1 in tubular epithelial cells increases cell proliferation.

The primary pathologic lesion associated with IRI in kidney transplantation is acute tubular necrosis, followed by tubular epithelial cell (TEC) regeneration.[23] However, kidney damage is not limited to TEC, and some studies also described podocyte loss after IRI.[3] There is controversy about the cellular sources of repair in tubular and glomerular injury.[24] Potential candidates are replication of surviving proximal TECs, clonal expansion of a small subset of proximal TECs, or cells of renin-lineage.[24] In addition, KPCs have been anticipated to be bona fide podocyte progenitors that play a relevant role in podocyte regeneration in health.[25] Moreover, it has recently been described that KPCs may promote proximal TEC regeneration after IRI in mice.[26] Thus, KPCs may be a suitable candidate for podocyte and TEC repair after IRI in kidney transplantation.

Epigenetic regulation of lineage-specific genes is a well-known mechanism for establishing cellular identity.[27] Hence, epigenetic reprogramming can mediate the regenerative or profibrotic response after kidney transplantation.[28] This epigenetic switch will depend on the environmental signals, including inflammation or myofibroblast activation and excess extracellular matrix.[29] IRI after kidney transplantation has also been described previously as an environmental factor influencing epigenetic modifications.[28,30,31] Hypoxia and oxidative stress after IRI cause DNA hypermethylation in the kidney allograft tissue, specifically

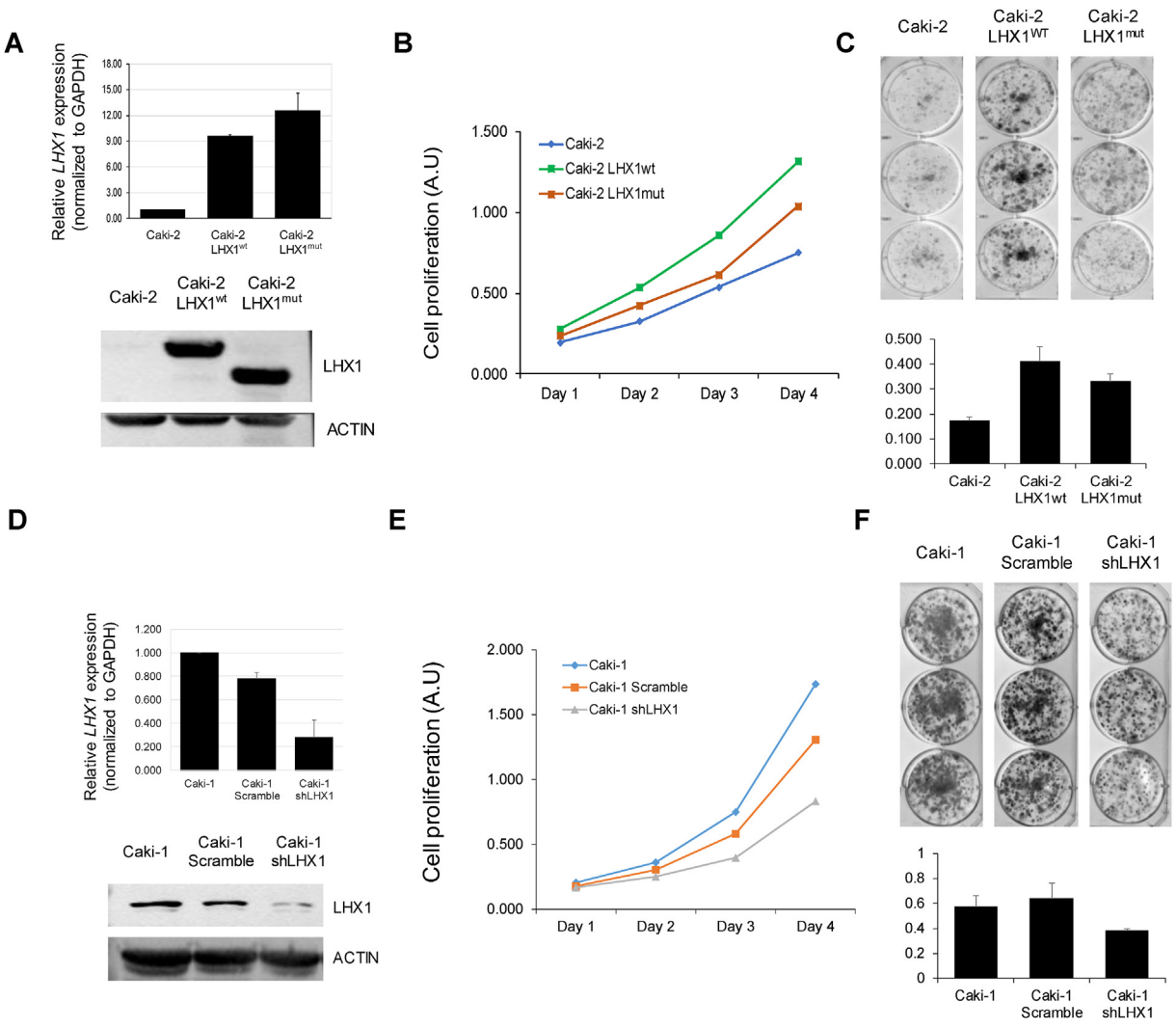

Figure 6. LIM homeobox-1 (LHX1) overexpression is associated with cellular proliferation in renal epithelial cell lines. **(**A) LHX1 expression was monitored using quantitative polymerase chain reaction (qPCR) (up) and western blot (down) in LHX1mut and LHX1wt-transfected Caki-2 cells. (B) Cell viability over time was determined using the 3-[4,5-dimethylthiazol-2-yl]-2,5 diphenyl tetrazolium bromide (MTT) assay after LHX1mut- and LHX1wt-transfection in Caki-2 cells. (C) Densitometric quantification and representative image of colonies of the colony-formation assay after LHX1mut- and LHX1wt-transfection in Caki-2 cells. (D) LHX1 expression was monitored using qPCR (up) and western blot (down) in short hairpin (sh)-scramble or sh-LHX1 transfected Caki-1 cells. (E) Cell viability over time was determined using the MTT assay after sh-LHX1 depletion in Caki-1 cells. (F) Densitometric quantification and representative image of colonies of the colony-formation assay after sh-LHX1 depletion in Caki-1 cells.

affecting some genes related to increased damage and fibrosis.[32] However, whether these changes are relevant in the specific population of KPCs is unknown. To encompass the clinical spectrum of IRI severity after kidney transplantation, we compared epigenetic and transcriptomics in U-KPCs obtained either after living or deceased donor transplantation. Our findings support the previous observation that severe IRI induces DNA methylation changes at specific genomic sequences in mice's kidney tissue[33] and those from Heylen et al[32] described in kidney biopsies. Nevertheless, our study provides new data regarding the epigenetic regulation of pathways involved in cellular repair in U-KPCs.

At the gene level, we identified hypermethylation of the *LHX1* promoter and consequently reduced gene expression after severe IRI. This gene is involved in the Mayer–Rokitansky–Küster–Hauser syndrome, in which upper urinary tract malformations are observed in about 40%, including unilateral renal agenesis, ectopia of one or both kidneys, renal hypoplasia, horseshoe kidneys, and hydronephrosis.[34] In mice, deletion of the LHX1 is associated with reduced number and small glomeruli, some of them immature or dysplastic.[35] LHX1 regulates the expression of foot process and podocyte junction-associated genes that result in podocyte differentiation.[36] According to all this evidence, our animal experiments showed that LHX1 is expressed in glomerular parietal epithelial cells, podocytes, and proximal TEC and a relationship between IRI severity, *LHX1* promoter hypermethylation, and *LHX1* gene expression. These results agreed with our observation in human U-KPCs, where severe ischemic damage (DD) was associated with lower LHX1 expression due to DNA hypermethylation. Our in vitro functional studies demonstrated that LHX1 overexpression is

associated with KPCs to podocyte differentiation and increased TEC proliferation, whereas LHX1 silencing is associated with decreased cell growth and proliferation. Overall, these new findings pave the way to further explore the specific role of the transcription factor LHX1 in different cell types and cellular environments.

Our findings of the epigenetic control of KPCs also provide clues on the long-term consequences of IRI. Like AKI to chronic kidney disease transition in native kidneys, delayed graft function is associated with kidney fibrosis and has a negative impact on long-term allograft function and survival.[37] IRI induces AKI and loss of nephrons that, depending on the severity of damage and the cell repair capacity, will account for glomerular hyperfiltration, podocyte detachment, proteinuria, progressive decline of glomerular filtration rate, and secondary focal segmental glomerulosclerosis (FSGS).[38,39] In native kidneys, a podocyte loss higher than 20% is required to induce KPC activation, migration, and FSGS.[40] Furthermore, podocyte stress causing accelerated podocyte detachment was described as a nonimmune mechanism of long-term allograft failure.[16,39] Our study provides new insights into the potential mechanisms connecting IRI with fibrosis in kidney allografts. IRI after kidney transplantation produces epigenetic and consequently transcriptional changes in $CD133^{+}CD24^{+}$ cells that may reduce their reparative capacity while inducing a profibrotic phenotype. This observation could be translated to the clinical setting, as FSGS is recognized as the most frequent pathologic lesion observed long-term after kidney transplantation.[41] Moreover, it has been reported that LHX1 inhibits tumor growth factor β1-induced epithelial-mesenchymal transition in renal tubular epithelial cells in mice.[42] Thus, LHX1 downregulation induced by severe IRI may enable epithelial-mesenchymal transition and contribute to the well-described clinicopathological correlation between delayed graft function and interstitial fibrosis and tubular atrophy in kidney transplantation.

Our study has some weaknesses and strengths. We used donor type as a surrogate marker of IRI severity, but other donor and recipient factors may play a role. However, similar findings were observed in a well-controlled experimental model of several times of kidney warm ischemia. We cannot rule out that culturing KPCs may induce methylation and gene expression changes in KPCs. Despite our results being highly innovative, there are still many issues to be solved for understanding the environmental signals that govern KPC reprogramming toward renal differentiation (tissue repair) or profibrotic response (tissue damage). Additional research regarding molecular pathways related to LHX1 is needed for specific therapeutic intervention. Several preclinical studies have shown that the use of drugs targeting DNA methylation (decitabine, hydrazine),[43,44] treatments with histone deacetylase inhibitors (SAHA, valproic acid),[45,46] or sirtuin activators (SRT-1720),[47] among others, reduce renal injury in AKI and chronic kidney disease models and promote renal repair. However, results are still controversial because of the heterogeneity of experimental models and the cellular targets. A better identification of the molecular mechanisms of response is essential to promoting the development of epigenetic therapies aimed at preventing renal failure after transplantation. Insights from future studies of KPCs and their epigenetic gene regulation in the process of renal differentiation may lead to new therapies for improving cellular repair after kidney damage.

Acknowledgments

The authors thank the staff of the Scientific and Technical Services at Barcelona University (Dr Esther Castaño, and Dr Benjamin Torrejón) for their help with sorter analysis and confocal microscopy. We thank the patients and their families. The authors thank the CERCA Programme/Generalitat de Catalunya for institutional support. The authors also thank the support from Instituto de Salud Carlos III (ISCIII)", RICORS2040, RD21/0005/0001 "Financiado por la Unión Europea – NextGeneration EU", Mecanismo para la Recuperación y la Resiliencia (MRR).

Funding

This study was supported by grants from the Instituto de Salud Carlos III co-funded by European Regional Development Funds (ERDF/FEDER) a way to build Europe (PI15/00638 and PI18/00910 to JMC and MB) and Generalitat de Catalunya (PERIS, SLT017/20/00074) and ERA PerMed JTC2021 PERNEPH (SLD078/21/000001).

Declaration of competing interest

The authors of this manuscript have no conflicts of interest to disclose as described by the American Journal of Transplantation.

Data availability

DNA methylation and RNA-sequencing data have been deposited in GEO and SRA public archives and are freely available under the accession GSE235814.

Appendix A. Supplementary data

Supplementary data to this article can be found online at https://doi.org/10.1016/j.ajt.2024.11.003.

ORCiD

Josep M. Cruzado https://orcid.org/0000-0003-1388-8558
Anna Sola https://orcid.org/0000-0003-2379-9313
Miguel L. Pato https://orcid.org/0000-0001-8840-7259
Anna Manonelles https://orcid.org/0000-0003-2456-388X
Cristian Varela https://orcid.org/0000-0001-5159-9592
Fernando E. Setién https://orcid.org/0000-0002-4061-4635
Carlos Quero-Dotor https://orcid.org/0000-0002-3951-2287
James S. Heald https://orcid.org/0000-0002-8095-0270
David Piñeyro https://orcid.org/0000-0001-5633-3339
Ana Amaya-Garrido https://orcid.org/0009-0008-6037-2638
Núria Doladé https://orcid.org/0000-0003-2311-2825
Sergi Codina https://orcid.org/0000-0002-2313-6109
Carlos Couceiro https://orcid.org/0000-0002-8303-8703

Núria Bolaños https://orcid.org/0000-0002-8340-6000
Montserrat Gomà https://orcid.org/0000-0003-0258-1526
Francesc Vigués https://orcid.org/0000-0003-3717-6301
Angelika Merkel https://orcid.org/0000-0001-5164-6803
Paola Romagnani https://orcid.org/0000-0002-1774-8088
María Berdasco https://orcid.org/0000-0002-6750-0400

References

1. Menke J, Sollinger D, Schamberger B, Heemann U, Lutz J. The effect of ischemia/reperfusion on the kidney graft. *Curr Opin Organ Transplant*. 2014;19(4):395–400. https://doi.org/10.1097/MOT.0000000000000090.
2. Nankivell BJ, Kuypers DRJ. Diagnosis and prevention of chronic kidney allograft loss. *Lancet*. 2011;378(9800):1428–1437. https://doi.org/10.1016/S0140-6736(11)60699-5.
3. Chen Y, Lin L, Tao X, Song Y, Cui J, Wan J. The role of podocyte damage in the etiology of ischemia-reperfusion acute kidney injury and post-injury fibrosis. *BMC Nephrol*. 2019;20(1):106. https://doi.org/10.1186/s12882-019-1298-x.
4. Codina S, Manonelles A, Tormo M, Sola A, Cruzado JM. Chronic kidney allograft disease: new concepts and opportunities. *Front Med (Lausanne)*. 2021;8:660334. https://doi.org/10.3389/fmed.2021.660334.
5. Schröppel B, Legendre C. Delayed kidney graft function: from mechanism to translation. *Kidney Int*. 2014;86(2):251–258. https://doi.org/10.1038/ki.2014.18.
6. Zhao L, Hu C, Han F, Cai F, Wang J, Chen J. Preconditioning is an effective strategy for improving the efficiency of mesenchymal stem cells in kidney transplantation. *Stem Cell Res Ther*. 2020;11(1):197. https://doi.org/10.1186/s13287-020-01721-8.
7. Osafune K. iPSC technology-based regenerative medicine for kidney diseases. *Clin Exp Nephrol*. 2021;25(6):574–584. https://doi.org/10.1007/s10157-021-02030-x.
8. McCampbell KK, Wingert RA. Renal stem cells: fact or science fiction? *Biochem J*. 2012;444(2):153–168. https://doi.org/10.1042/BJ20120176.
9. Bruno S, Chiabotto G, Camussi G. Concise review: different mesenchymal stromal/stem cell populations reside in the adult kidney. *Stem Cells Transl Med*. 2014;3(12):1451–1455. https://doi.org/10.5966/sctm.2014-0142.
10. Sagrinati C, Netti GS, Mazzinghi B, et al. Isolation and characterization of multipotent progenitor cells from the Bowman's capsule of adult human kidneys. *J Am Soc Nephrol*. 2006;17(9):2443–2456. https://doi.org/10.1681/ASN.2006010089.
11. Eng DG, Sunseri MW, Kaverina NV, Roeder SS, Pippin JW, Shankland SJ. Glomerular parietal epithelial cells contribute to adult podocyte regeneration in experimental focal segmental glomerulosclerosis. *Kidney Int*. 2015;88(5):999–1012. https://doi.org/10.1038/ki.2015.152.
12. Smeets B, Kuppe C, Sicking EM, et al. Parietal epithelial cells participate in the formation of sclerotic lesions in focal segmental glomerulosclerosis. *J Am Soc Nephrol*. 2011;22(7):1262–1274. https://doi.org/10.1681/ASN.2010090970.
13. Lazzeri E, Ronconi E, Angelotti ML, et al. Human urine-derived renal progenitors for personalized modeling of genetic kidney disorders. *J Am Soc Nephrol*. 2015;26(8):1961–1974. https://doi.org/10.1681/ASN.2014010057.
14. Rahman MS, Wruck W, Spitzhorn L-S, et al. The FGF, TGFβ and WNT axis modulate self-renewal of human six2+ urine derived renal progenitor cells. *Sci Rep*. 2020;10(1):739. https://doi.org/10.1038/s41598-020-57723-2.
15. Arcolino FO, Zia S, Held K, et al. Urine of preterm neonates as a novel source of kidney progenitor cells. *J Am Soc Nephrol*. 2016;27(9):2762–2770. https://doi.org/10.1681/ASN.2015060664.
16. Manonelles A, Guiteras R, Melilli E, et al. The presence of urinary renal progenitor cells in stable kidney transplant recipients anticipates allograft deterioration. *Front Physiol*. 2018;9:1412. https://doi.org/10.3389/fphys.2018.01412.
17. Liu WB, Huang GR, Liu BL, et al. Single cell landscape of parietal epithelial cells in healthy and diseased states. *Kidney Int*. 2023;104(1):108–123. https://doi.org/10.1016/j.kint.2023.03.036.
18. Cheah SS, Kwan KM, Behringer RR. Requirement of LIM domains for LIM1 function in mouse head development. *Genesis*. 2000;27(1):12–21. https://doi.org/10.1002/1526-968X(200005)27:1<12::AID-GENE30>3.0.CO;2-X.
19. Berger K, Bangen J-M, Hammerich L, et al. Origin of regenerating tubular cells after acute kidney injury. *Proc Natl Acad Sci U S A*. 2014;111(4):1533–1538. https://doi.org/10.1073/pnas.1316177111.
20. Glube N, Giessl A, Wolfrum U, Langguth P. Caki-1 cells represent an in vitro model system for studying the human proximal tubule epithelium. *Nephron Exp Nephrol*. 2007;107(2):e47–56. https://doi.org/10.1159/000107804.
21. Cirio MC, Hui Z, Haldin CE, et al. Lhx1 is required for specification of the renal progenitor cell field. *PLoS One*. 2011;6(4):e18858. https://doi.org/10.1371/journal.pone.0018858.
22. Dormoy V, Béraud C, Lindner V, et al. LIM-class homeobox gene Lim1, a novel oncogene in human renal cell carcinoma. *Oncogene*. 2011;30(15):1753–1763. https://doi.org/10.1038/onc.2010.557.
23. Kellum JA, Romagnani P, Ashuntantang G, Ronco C, Zarbock A, Anders H-J. Acute kidney injury. *Nat Rev Dis Primers*. 2021;7(1):52. https://doi.org/10.1038/s41572-021-00284-z.
24. Naved BA, Bonventre JV, Hubbell JA, et al. Kidney repair and regeneration: perspectives of the NIDDK (Re)Building a Kidney consortium. *Kidney Int*. 2022;101(5):845–853. https://doi.org/10.1016/j.kint.2022.02.023.
25. Bronstein R, Pace J, Gowthaman Y, Salant DJ, Mallipattu SK. Podocyte-parietal epithelial cell interdependence in glomerular development and disease. *J Am Soc Nephrol*. 2023;34(5):737–750. https://doi.org/10.1681/ASN.0000000000000104.
26. Hong X, Nie H, Deng J, et al. $WT1^+$ glomerular parietal epithelial progenitors promote renal proximal tubule regeneration after severe acute kidney injury. *Theranostics*. 2023;13(4):1311–1324. https://doi.org/10.7150/thno.79326.
27. Berdasco M, Esteller M. Aberrant epigenetic landscape in cancer: how cellular identity goes awry. *Dev Cell*. 2010;19(5):698–711. https://doi.org/10.1016/j.devcel.2010.10.005.
28. Guo C, Dong G, Liang X, Dong Z. Epigenetic regulation in AKI and kidney repair: mechanisms and therapeutic implications. *Nat Rev Nephrol*. 2019;15(4):220–239. https://doi.org/10.1038/s41581-018-0103-6.
29. Black LM, Lever JM, Agarwal A. Renal Inflammation and fibrosis: a double-edged sword. *J Histochem Cytochem*. 2019;67(9):663–681. https://doi.org/10.1369/0022155419852932.
30. Xiang X, Zhu J, Dong G, Dong Z. Epigenetic regulation in kidney transplantation. *Front Immunol*. 2022;13:861498. https://doi.org/10.3389/fimmu.2022.861498.
31. Tang J, Zhuang S. Histone acetylation and DNA methylation in ischemia/reperfusion injury. *Clin Sci (Lond)*. 2019;133(4):597–609. https://doi.org/10.1042/CS20180465.
32. Heylen L, Thienpont B, Naesens M, et al. Ischemia-induced DNA hypermethylation during kidney transplant predicts chronic allograft injury. *J Am Soc Nephrol*. 2018;29(5):1566–1576. https://doi.org/10.1681/ASN.2017091027.
33. Zhao Y, Ding C, Xue W, et al. Genome-wide DNA methylation analysis in renal ischemia reperfusion injury. *Gene*. 2017;610:32–43. https://doi.org/10.1016/j.gene.2017.02.005.
34. Herlin MK, Petersen MB, Brännström M. Mayer-Rokitansky-Küster-Hauser (MRKH) syndrome: a comprehensive update. *Orphanet J Rare Dis*. 2020;15(1):214. https://doi.org/10.1186/s13023-020-01491-9.
35. Warren EB, Briano JA, Ellegood J, DeYoung T, Lerch JP, Morrow EM. 17q12 deletion syndrome mouse model shows defects in craniofacial,

brain and kidney development, and glucose homeostasis. *Dis Model Mech*. 2022;15(12):dmm049752. https://doi.org/10.1242/dmm.049752.
36. Tomar R, Mudumana SP, Pathak N, Hukriede NA, Drummond IA. osr1 is required for podocyte development downstream of wt1a. *J Am Soc Nephrol*. 2014;25(11):2539–2545. https://doi.org/10.1681/ASN.2013121327.
37. Swanson KJ, Bhattarai M, Parajuli S. Delayed graft function: current status and future directions. *Curr Opin Organ Transplant*. 2023;28(1):1–7. https://doi.org/10.1097/MOT.0000000000001034.
38. Cruzado JM, Torras J, Riera M, et al. Influence of nephron mass in development of chronic renal failure after prolonged warm renal ischemia. *Am J Physiol Renal Physiol*. 2000;279(2):F259–F269. https://doi.org/10.1152/ajprenal.2000.279.2.F259.
39. Yang Y, Hodgin JB, Afshinnia F, et al. The two kidney to one kidney transition and transplant glomerulopathy: a podocyte perspective. *J Am Soc Nephrol*. 2015;26(6):1450–1465. https://doi.org/10.1681/ASN.2014030287.
40. Wharram BL, Goyal M, Wiggins JE, et al. Podocyte depletion causes glomerulosclerosis: diphtheria toxin-induced podocyte depletion in rats expressing human diphtheria toxin receptor transgene. *J Am Soc Nephrol*. 2005;16(10):2941–2952. https://doi.org/10.1681/ASN.2005010055.
41. Stegall MD, Cornell LD, Park WD, Smith BH, Cosio FG. Renal allograft histology at 10 years after transplantation in the tacrolimus era: evidence of pervasive chronic injury. *Am J Transplant*. 2018;18(1):180–188. https://doi.org/10.1111/ajt.14431.
42. Li X, Wu N, Chen Y, et al. Degradation of different molecular weight fucoidans and their inhibition of TGF-β1 induced epithelial-mesenchymal transition in mouse renal tubular epithelial cells. *Int J Biol Macromol*. 2020;151:545–553. https://doi.org/10.1016/j.ijbiomac.2020.02.068.
43. Li Z, Li N. Epigenetic Modification drives acute kidney injury-to-chronic kidney disease progression. *Nephron*. 2021;145(6):737–747. https://doi.org/10.1159/000517073.
44. Tampe B, Steinle U, Tampe D, et al. Low-dose hydralazine prevents fibrosis in a murine model of acute kidney injury-to-chronic kidney disease progression. *Kidney Int*. 2017;91(1):157–176. https://doi.org/10.1016/j.kint.2016.07.042.
45. Costalonga EC, Silva FMO, Noronha IL. Valproic acid prevents renal dysfunction and inflammation in the ischemia-reperfusion injury model. *Biomed Res Int*. 2016;2016:5985903. https://doi.org/10.1155/2016/5985903.
46. Fan H, Yang H-C, You L, Wang Y-Y, He W-J, Hao C-M. The histone deacetylase, SIRT1, contributes to the resistance of young mice to ischemia/reperfusion-induced acute kidney injury. *Kidney Int*. 2013;83(3):404–413. https://doi.org/10.1038/ki.2012.394.
47. Ren Y, Du C, Shi Y, Wei J, Wu H, Cui H. The Sirt1 activator, SRT1720, attenuates renal fibrosis by inhibiting CTGF and oxidative stress. *Int J Mol Med*. 2017;39(5):1317–1324. https://doi.org/10.3892/ijmm.2017.2931.